

Combinatorial Optimization of Engineering Systems based on Diagrammatic Design

VOLODYMYR RIZNYK
 Lviv Polytechnic National University,
 79013, Lviv-13, Stepan Bandera Str., 12,
 UKRAINE

Abstract: - The objectives of the combinatorial optimization of engineering systems based on diagrammatic design are enhancing technical indices of the systems with spatially or temporally distributed elements (e.g., radio-antenna arrays) concerning resolving ability, positioning precision, transmission speed, and performance reliability, using the graphical performance of appropriate algebraic models of the system, such as cyclic difference sets, Galois fields and “Ideal Ring Bundles”. The diagrammatic design provides configuring systems with a smaller number of elements than at present, while upholding or improving on the other significant operating quality indices of the system.

Key-Words: - non-uniform structure, spiral diagram, Galois field, Ideal Ring Bundle, combinatorial optimization, design technique, quality indices, high-performance cyclic code, optimized self-correcting code.

Received: October 23, 2023. Revised: April 9, 2024. Accepted: May 24, 2024. Published: July 1, 2024.

1 Introduction

In the last few years modern circuit and system engineering have wide world gratitude for finding optimal technological solutions using combinatorial optimization of devices or systems based on mathematical principles of the system design. This article devotes solving technological problems referring to structural optimization of engineering devices or systems, using theory of combinatorial configurations, [1], [2], [3], [4], including such algebraic constructions as cyclic difference sets [5], [6], [7], [8], projective planes [9], [10], finite field theory [11], [12], [13], and concept of the Ideal Ring Bundles (IRBs), [14].

2 Problem Formulation

The very important problem for innovative system engineering is finding the optimal placement of structural elements in spatially or temporally distributed systems, including two- and multidimensional structures of the system.

3 Problem Solution

Finding optimal solutions for wide classes of technological problems requires the application of combinatorial design techniques, using profitable cyclic ordered numerical or vector diagrams of

Galois fields [11], [12], [13] and Ideal Ring Bundles [14]. The task is to increase transmission speed, positioning accuracy, resolving ability, vector signal coding, data compressing, and functionality of engineering devices or systems.

3.1 Ideal Ring Sequences

To the study of combinatorial properties of ring sequences of positive integers let us calculate all sums of connected sub-sequences of the sequence. Sums of connected elements on ring ordered n -stage sequence $K = \{k_1, k_2, \dots, k_n\}$ are given in Table 1.

Table 1. Sums of connected elements of ring ordered n -stage sequence $K = \{k_1, k_2, \dots, k_n\}$

$K = \{k_1, k_2, \dots, k_n\}$					
P_j	q_j				
	1	2	...	$n-1$	n
1	k_1	$\sum_{i=1}^2 k_i$...	$\sum_{i=1}^{n-1} k_i$	$\sum_{i=1}^n k_i$
2	$\sum_{i=1}^n k_i$	k_2	...	$\sum_{i=2}^{n-1} k_i$	$\sum_{i=2}^n k_i$
...
$n-1$	$\sum_{i=n-1}^n k_i + k_1$	$\sum_{i=n-1}^n k_i + \sum_{i=1}^2 k_i$...	k_{n-1}	$\sum_{i=n-1}^n k_i$
n	$k_n + k_1$	$k_n + \sum_{i=1}^2 k_i$...	$\sum_{i=1}^n k_i$	k_n

Coordinates (p_j, q_j) correspond to appropriate sum of connected elements (p_j, q_j) of a ring-ordered n -stage sequence.

If $p_j = q_j$, a ring sum is equal to k_i ; in case p_j

$< q_j$ it is $\sum_{i=p_j}^{q_j} k_i$; or $\sum_{i=1}^{q_j} k_i + \sum_{i=p_j}^n k_i$ for $p_j > q_j$.

In Table 1 the maximum number of *distinct* sums S of connected elements of a ring-ordered n -stage sequence is given by:

$$S = n^2 - n + 1 \tag{1}$$

If a sum of any number of connected elements in the sequence enumerate the set of integers from 1 to S , we call this “ideal” ring sequence, shortly, Ideal Ring (IR) with parameters S and n .

Now we see an example of an IR with $S=13$, $n=4$, namely $\{1, 3, 2, 7\}$. Here we observe:

1=1	5=3+2	9 = 2+7	13= 1+3+2+7
2=2	6=1+3+2	10= 2+7+1	
3=3	7=7	11= 7+1+3	
4=1+3	8=7+ 1	12=3+2+7	

One more variant of IRs with the same parameters $S=13$, $n=4$ is four-stage cyclic sequence $\{1, 2, 6, 4\}$:

1=1	5=4+1	9 = 1+2+6	13= 1+2+6+4
2=2	6=6	10= 6+4	
3=1+2	7=4+1+2	11= 6+4+1	
4=4	8= 2 + 6	12=2+6+4	

Theoretically, there are numerous Ideal Rings.

4 Graphic Design of Ideal Rings

4.1 One-dimensional Ideal Rings

One-dimensional Ideal Rings (IRs) are numerical cyclic sequences of arbitrary one-dimensional elements (e.g., parts of a set), which can be presented graphically as a wreath of the elements. Here is a chart of the IR $\{1, 3, 2, 7\}$ (Figure 1).

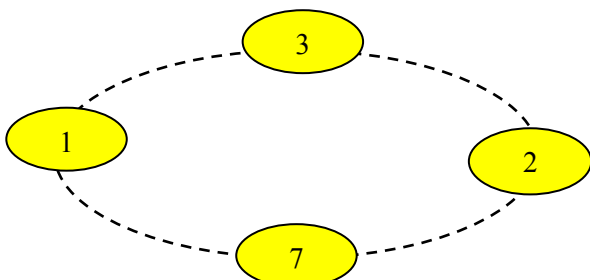


Fig. 1: A chart of the IR $\{1, 3, 2, 7\}$

Easy to see, that if summing over more than one complete revolving around the ring, you can obtain all integers as such sums:

$14= 1+3+2+7+1$, $15= 2+7+1+3+2$, $16= 3+2+7+1+3$, etc.

A numerical spiral diagram of the IR $\{1, 3, 2, 7\}$ is given below (Figure 2).

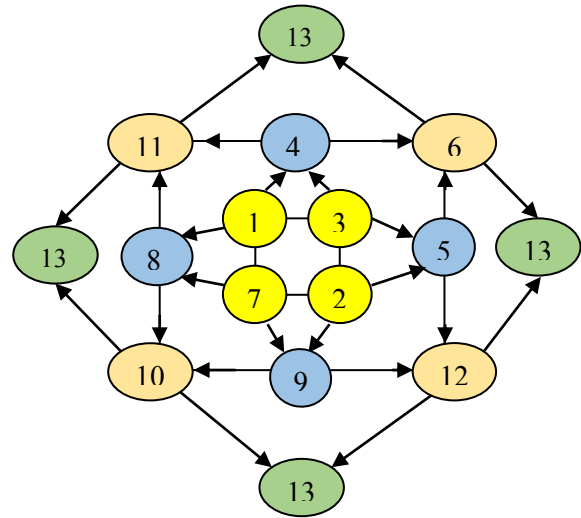


Fig. 2: Numerical spiral diagram of the IR $\{1, 3, 2, 7\}$

The numerical diagram (Figure 2) consists of four-stage ($n = 4$) ring sequences placed one inside another, so that the inner sequence is the IRB $\{1, 3, 2, 7\}$ (yellow beads), and it forms the rest of the ring sequences by summing of its consecutive terms from 2 to 4, namely: $\{4, 5, 9, 8\}$ (blue beads), $\{6, 12, 10, 11\}$ (orange beads), and finally $\{13, 13, 13, 13\}$. The arrows point the direction of the summing and give a place for circular sum's arrangement in the spiral-like diagram. We can find this each ring sum from 1 to $n(n - 1) = 12$ occurring exactly once on the diagram. Using equation (1) easy to calculate a maximum number of distinct sums S of any IRB: 3, 7, 13, 21, 31, etc. We say this numerical set is a generative IRBs row for configure numerical spiral diagram of any ring ordered n -stage sequence of the IRB.

A chart of the IR $\{1, 2, 6, 4\}$ is depicted in Figure 3.

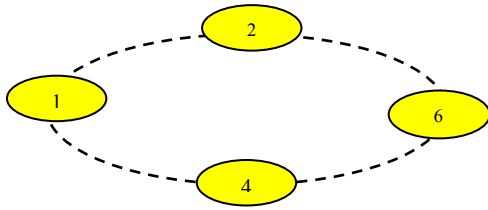


Fig. 3: A chart of the IR {1, 2, 6, 4}

Numerical spiral diagram of the IR {1, 2, 6, 4} is presented in Figure 4.

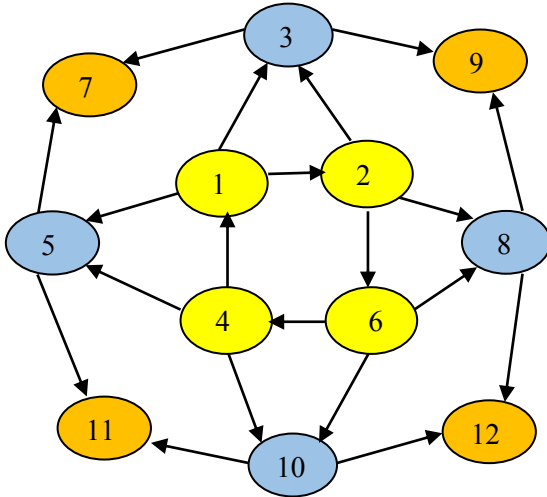


Fig. 4: Numerical spiral diagram of the IR {1, 2, 6, 4}

Spiral diagram (Figure 4) consists of four-stage ($n=4$) ring sequences placed one inside another, so that the inner sequence is the IRB {1, 2, 6, 4} (yellow beads), and it forms the rest of the ring sequences by summing of its consecutive terms from 2 to 4, namely: {3, 8, 10, 5} (blue beads), and {7, 9, 12, 11} (orange beads). The arrows point the direction of the summing and give a place for circular sum's arrangement in the spiral-like diagram. We can find this each ring sum from 1 to n ($n - 1$) = 12 occurring exactly once on the diagram.

4.2 Ideal Ring Bundles in Extension of Galois Fields

Researches into the underlying diagrammatic design involve the graphic presentation of cyclic groups in extensions of Galois fields, [11], [12]. A graphic rotational scheme in $GF(3^2)$ of the Ideal Ring {1,2,6,4} with parameters $S=13$ and $n = 4$, is given in Figure 5.

Let us regard model of optimum rotational device as (4, 13)-IRB in terms of Galois theory. In this case prime element x of $GF(3^2)$ satisfies equation $f(x)=x^3-x-1$. Here $f(x)$ is polynomial irreducible over $GF(3^2)$, where $p=3$, and $m=2$ (Fig.3).

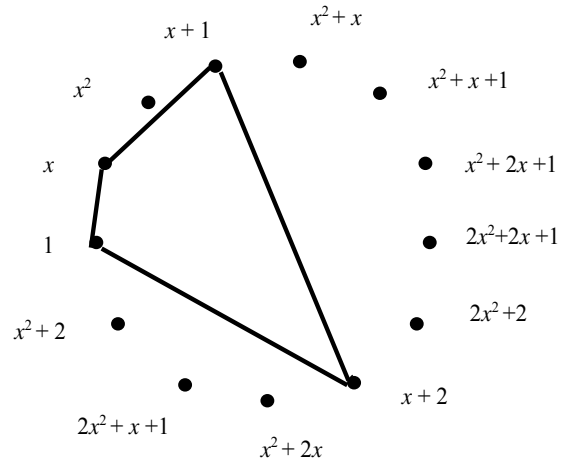


Fig. 5: A graphic rotational scheme in $GF(3^2)$ of the Ideal Ring {1,2,6,4} with parameters $S=13$ and $n = 4$

Prime elements x of $GF(3^2)$ satisfy equation $f(x)=x^3-x-1$, where $f(x)$ is 3-degree polynomial irreducible over $GF(3^2)$, $p=3$, $m=2$:

$$\begin{aligned}
 x^0 &\equiv 1 \\
 x^1 &\equiv x \\
 x^2 &\equiv x^2 \\
 x^3 &\equiv x+1 \\
 x^4 &\equiv x^2+x \\
 x^5 &\equiv x^2+x+1 \\
 x^6 &\equiv x^2+2x+1 \\
 x^7 &\equiv 2x^2+2x+1 \\
 x^8 &\equiv 2x^2+2 \\
 x^9 &\equiv x+2 \\
 x^{10} &\equiv x^2+2x \\
 x^{11} &\equiv 2x^2+x+1 \\
 x^{12} &\equiv x^2+2
 \end{aligned}
 \left. \vphantom{\begin{aligned} x^0 &\equiv 1 \\ x^1 &\equiv x \\ x^2 &\equiv x^2 \\ x^3 &\equiv x+1 \\ x^4 &\equiv x^2+x \\ x^5 &\equiv x^2+x+1 \\ x^6 &\equiv x^2+2x+1 \\ x^7 &\equiv 2x^2+2x+1 \\ x^8 &\equiv 2x^2+2 \\ x^9 &\equiv x+2 \\ x^{10} &\equiv x^2+2x \\ x^{11} &\equiv 2x^2+x+1 \\ x^{12} &\equiv x^2+2 \end{aligned}} \right\} \pmod{3, x^3-x-1}$$

The graphic scheme (Figure 6) displays two non-uniform polygons of four ($n_1=4$), and nine ($n_2=9$) vertexes as the $GF(3^2)$:

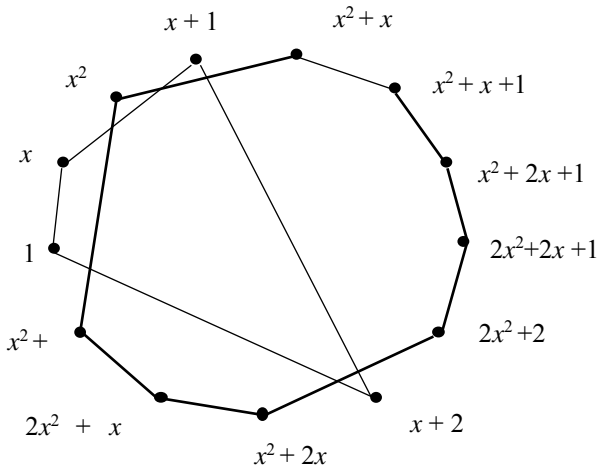


Fig. 6: Graphic scheme of two non-uniform polygons of four ($n_1=4$), and nine ($n_2=9$) vertices as the $GF(3^2)$

To see this, we observe representation of two complementary IRBs. The first of them placed in the vertexes x^0, x^1, x^3, x^9 is the IRB $\{1, 2, 6, 4\}$ with $S=13, n=4$, while the second – in vertexes $x^2, x^4, x^5, x^6, x^7, x^8, x^{10}, x^{11}, x^{12}$ starting the IRB $\{2,1,1,1,1,2,1,1,3\}$ with $n=9$, where ring sums of the IRB enumerate the set of integers $[1, S - 1]$ exactly 6-times. Graphic scheme (Figure 6) allows combinatorial optimization of engineering devices or systems based on wonderful geometric and pictorial properties of Galois fields in rotational symmetry graphical presentation.

4.3 Diagrammatic of Two-dimensional Ideal Ring Bundles

Next, we regard the n -stage ring sequence $K_{2D} = \{(k_{11}, k_{12}), (k_{21}, k_{22}), \dots, (k_{n1}, k_{n2}), \dots, (k_{n1}, k_{n2})\}$, where we require all terms in each circular vector-sum to be consecutive 2-stage sequences as elements of the sequence. Example: IRB containing four ($n=4$) two-dimensional (2-D) elements: $k_1=(0,2), k_2=(1,3), k_3=(0,1), k_4=(2,3)$ is depicted in the diagram (Figure 7).

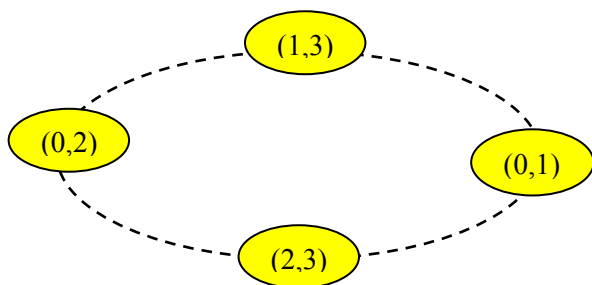


Fig. 7: Diagram of the 2-D IRB

$$\{(0,2), (1,3), (0,1), (2,3)\}$$

Easy to calculate all 2-D vector-sums of the 2-D IRB $\{(0,2), (1,3), (0,1), (2,3)\}$, taking twice modulo $m_1 = n - 1 = 3$, and $m_2 = n = 4$ correspondently:

$$\begin{aligned} (1,0) &\equiv (0,1) + (1,3); \\ (1,1) &\equiv (1,3) + (0,2); & (2,1) &\equiv (0,2) + (2,3); \\ (2,0) &\equiv (2,3) + (0,1); \\ (1,2) &\equiv (0,1) + (1,3) + (0,2); & (2,2) &\equiv (0,2) + (2,3) + (0,1); \\ (0,3) &\equiv (2,3) + (0,1) + (1,3); & (0,0) &\equiv (1,3) + (0,2) + (2,3). \end{aligned}$$

Vector-sums of the 2-D IRB $\{(0,2), (1,3), (0,1), (2,3)\}$, taking twice modulo $m_1 = n - 1 = 3$, and $m_2 = n = 4$ is given in Table 2.

Table 2. Vector-sums of the 2-D IRB $\{(0,2), (1,3), (0,1), (2,3)\}$, taking twice modulo $m_1 = n - 1 = 3, m_2 = n = 4$

Vector-sums	Basic vectors			
(0,0)	(0,2)	(1,3)	-	(2,3)
(0,1)	-	-	(0,1)	-
(0,2)	(0,2)	-	-	-
(0,3)	-	(1,3)	(0,1)	(2,3)
(1,0)	-	(1,3)	(0,1)	-
(1,1)	(0,2)	(1,3)	-	-
(1,2)	(0,2)	(1,3)	(0,1)	-
(1,3)	-	(1,3)	-	-
(2,0)	-	-	(0,1)	(2,3)
(2,1)	(0,2)	-	-	(2,3)
(2,2)	(0,2)	-	(0,1)	(2,3)
(2,3)	-	-	-	(2,3)

These basic vectors $\{(0,2), (1,3), (0,1), (2,3)\}$ of the ring sequence themselves are circular 2-D vector-sums too, forming a coordinate system of size 3×4 over the surface of the torus:

$$\begin{matrix} (2,0) & (2,1) & (2,2) & (2,3) \\ (1,0) & (1,1) & (1,2) & (1,3) \\ (0,0) & (0,1) & (0,2) & (0,3) \end{matrix}$$

Here is an example of the 2-D IR $\{(0,2), (1,3), (0,1), (2,3)\}$ vector ring as colored diagram (Figure 8).

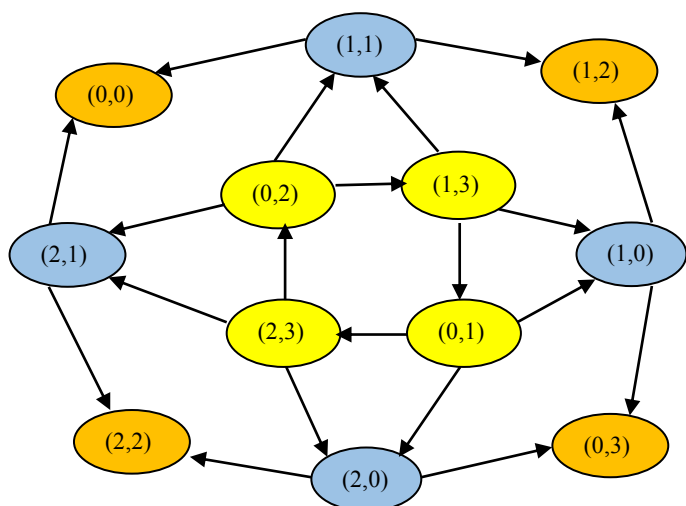


Fig. 8: Vector ring diagram of the 2-D IRB $\{(0,2), (1,3), (0,1), (2,3)\}$

Diagram (Figure 8) consists of four ($n=4$) n -stage ring sequences of 2-D vectors, placed one inside another so that the inner sequence is the 2-D IRB $\{(0,2), (1,3), (0,1), (2,3)\}$ (yellow beads). It forms the rest of the ring sequences by summing modulo 3 and 4 of its consecutive 2-D vectors $\{(1,1), (1,0), (2,0), (2,1)\}$ (blue beads), and finally $\{(1,2), (0,3), (2,2), (0,0)\}$ (orange beads). The arrows point direction of the summing giving locations of all modular sums in the ring diagram. We can observe that each modular sum from (0,0) to (2,3) occurs exactly once on the diagram.

The result of the computation forms two-dimensional grid over torus 3×4 , where 2-D modular coordinates of each node of the grid enumerated exactly once. Hence, the ring vector sequence $\{(0,2), (1,3), (0,1), (2,3)\}$ is two-dimensional ($t=2$) Ideal Ring Bundle with $S=13$, $n=4$, $m_1=3$, $m_2=4$. The IRB forms two-dimensional coordinate grid over surface of torus $m_1 \times m_2$. Here each node point of the coordinate grid occurs exactly once, as well as it creates binary 4-digit ($n=4$) two-dimensional code with the weighted bits $\{(0,2), (1,3), (0,1), (2,3)\}$ under intelligent torus coordinate system 3×4 , where $m_1=3$, $m_2=4$ (Table 3).

Table 3 contains 12 binary four-digit ($n = 4$) combinations ($n^2 - n = 12$) for coding two attributes ($t = 2$) both with three ($m_1 = 3$) categories of the first, and four ($m_2=4$) – the second attributes concurrently.

Table 3. Binary 2-D vector code based on the IRB $\{(0,2), (1,3), (0,1), (2,3)\}$

The 2-D IRB code under the torus coordinate system $m_1 \times m_2 = 3 \times 4$					
No	Vector	Digit weights of the 2-D code			
		(0,2)	(1,3)	(0,1)	(2,3)
1	(0,0)	1	1	0	1
2	(0,1)	0	0	1	0
3	(0,2)	1	0	0	0
4	(0,3)	0	1	1	1
5	(1,0)	0	1	1	0
6	(1,1)	1	1	0	0
7	(1,2)	1	1	1	0
8	(1,3)	0	1	0	0
9	(2,0)	0	0	1	1
10	(2,1)	1	0	0	1
11	(2,2)	1	0	1	1
12	(2,3)	0	0	0	1

5 Discussion

As is evident from Table 1 and equation (1), combinatorial properties of n -stage ring sequences of positive integers allows the enumeration of all sums of connected sub-sequences of the sequence in a finite interval $[1, n^2 - n + 1]$. We call this Ideal Ring Bundles (IRBs). Chart of IRB $\{1, 3, 2, 7\}$ is given in Figure 1. Numerical spiral diagram of the IRB (Figure 2) demonstrates the structural perfection of the combinatorial configuration. It consists of four-stage ($n=4$) ring sequences placed one inside another so that the inner sequence is the IRB. Chart of IRB $\{1, 2, 6, 4\}$ is given in Figure 3, and its numerical spiral diagram of the IRB (Figure 4) well evident existing isomorphic constructions of IRBs, as well as combinatorial varieties of them. These diagrammatic schemes emulate designing engineering devices or systems with optimal spatially or temporally distributed structural elements of the system. A graphic rotational scheme (Figure 5) allows the optimization of engineering systems using diagrammatic design in Galois fields. The graphic scheme (Figure 6) displays two non-uniform polygons of four ($n_1=4$), and nine ($n_2=9$) vertexes as the $GF(3^2)$. The first of them form IRB $\{1, 2, 6, 4\}$, where each rings the second matches IRB 9-polygon, where each ring sums from 1 to $S - 1 = 11$ occurs exactly once, while sums enumerate the same set of integers exactly 9-times. The last types of IRBs make it

possible to configure optimized coding systems, which provide an opportunity to detect up to 50 % or correct up to 25 % errors of code combination length with rising n to ∞ asymptotically [14]. A diagram (Figure 7) demonstrates forming a coordinate system of size 3×4 over the surface of a torus based on the 2-D IRB $\{(0,2), (1,3), (0,1), (2,3)\}$ (Table 2). Diagram (Figure 8) consists of four 4-stage ring sequences of 2-D vectors, placed one inside another, so that the inner four sequences are these basic vectors. Table 3 presents an example of binary two-dimensional code words with the weighted bits $\{(0,2), (1,3), (0,1), (2,3)\}$, which consist of no more than one monolithic part both of bits “1” or “0” in code combinations as being cyclic. Theoretically, there are infinitely many varieties of useful combinatorial configurations for the optimization of engineering systems based on diagrammatic design. Such an approach to be profitable for combinatorial optimization of a number of technological problems, e.g., high-performance error-corrected encoding systems, self-correcting monolithic codes, and multidimensional information manifold coordinate systems for data processing attribute sets at the same time without of parallel computation, [14].

6 Conclusion

The essence of the proposed project technology is combinatorial optimization of engineering systems based on diagrammatic design for enhancing technical indices of the systems with spatially or temporally distributed elements. Because diagrams and graphs are clear and easy to read and understand, the study of diagrammatic reasoning is about the understanding of concepts and ideas, visualized with the use of the diagrams and imagery. Diagrammatic and graphic presentation of data means visual representation of the data. It shows a comparison between two or more sets of data and helps in the presentation of highly complex data, e.g., geometric relationships of cyclic groups in extensions of Galois fields, helping design of optimized engineering systems. Diagrams and graphs are clear and easy to read and understand. The modern circuit and system engineering have wide world gratitude connecting fast development in the field of system engineering, information technologies, and radio-electronics. Combinatorial optimization of engineering systems

based diagrammatic design make it possible to configure structure of the systems with the smaller number of elements than at present, whereas upholding or improving on the other significant operating quality indices of the system.

References:

- [1] M.Jr. Hall, *Combinatorial Theory*: Wiley-Interscience, 1998, p.464, DOI: 10.1002 / 978111803286.
- [2] Mitchel T.Keller, William T.Trotter, *Applied Combinatorics*, 2017, p.393.
- [3] Lorenz J.Halbeisen, *Combinatorial Set Theory*. Second Edition: Springer, 2017, p.610.
- [4] Edwin E. Beckenbach, *Applied Combinatorial Mathematics*, John Wiley and Sons, Inc. New York, London, Sidney, 1964.
- [5] Baumert Leonard D. Cyclic difference sets. *Lecture Notes in Mathematics*, Vol. 182 Springer - Verlag, Berlin-New York 1971.
- [6] Moore, EH; Pollastek, HSK, "Difference Sets: Connecting Algebra, Combinatorics, and Geometry", 2013. AMS. ISBN: 978-0-8218-9176-6.
- [7] M. Buratti, Hadamard partitioned difference families and their descendants, *Cryptogr. Commun.*, 11 (2019), p.557-562. doi: 10.1007/s12095-018-0308-3.
- [8] Jungnickel, D., Pott, A., Smith, K.W: Difference sets. In: Colbourn, C.J., Dinitz, J.H. (eds.) *Handbook of Combinatorial Designs*. 2nd edn., pp 419–435. Chapman & Hall/CRC, Boca Raton (2006)
- [9] Stevenson, Frederick W. (1972), *Projective Planes*, San Francisco: W.H. Freeman and Company, ISBN: 0-7167-0443-9.
- [10] Weintraub, Steven H. (1978), "Group actions on homology quaternionic projective planes", *Proceedings of the American Mathematical Society*, 70, p.75-82.
- [11] Joseph Rotman, *Galois Theory* (Second ed.): Springer, 1998, doi: 10.1007/978-1-4612-0617-0, ISBN: 0-387-98541-7. MR 164558.
- [12] Cunxi Yu, and Maciej Ciesielski, "Formal Analysis of Galois Field Arithmetic Circuits - Parallel Verification and Reverse Engineering," in *EEE Transactions on Computer-Aided Design of Integrated Circuits and Systems*, 2018, vol. 38, Issue 2, pp.354-365, DOI: 10.1109/TCAD.2018.2808457T.

- [13] Pruss, P. Kalla, and F. Enescu, "Efficient symbolic computation for word-level abstraction from combinational circuits for verification over finite fields", *IEEE Trans. Comput. -Aided Design Integr. Circuits Syst.*, vol. 35, no. 7, pp. 1206-1218, Jul. 2016.
- [14] V.Riznyk, Optimization of Encoding Design Based on the Spatial Geometry Remarkable Properties, *WSEAS Transactions on Computers*, Vol.20, pp.270-276, <https://doi.org/10.37394/23205.2022.21.33>.

Contribution of Individual Authors to the Creation of a Scientific Article (Ghostwriting Policy)

The author contributed in the present research, at all stages from the formulation of the problem to the final findings and solution.

Sources of Funding for Research Presented in a Scientific Article or Scientific Article Itself

No funding was received for conducting this study.

Conflict of Interest

The authors have no conflicts of interest to declare.

Creative Commons Attribution License 4.0 (Attribution 4.0 International, CC BY 4.0)

This article is published under the terms of the Creative Commons Attribution License 4.0

https://creativecommons.org/licenses/by/4.0/deed.en_US